In-situ Assessment and Comparison of the Thermal Performance of Three Building Envelopes in a Nordic Climate

Luigiano Duarte,[a,b,*] Pierre Blanchet ,[a,*] Lara Ramadan,[b] and Richard Trempe [c]

** Corresponding authors: luigiano.duarte.1@ulaval.ca; pierre.blanchet@sbf.ulaval.ca*

DOI: 10.15376/biores.21.1.1645-1668

GRAPHICAL ABSTRACT

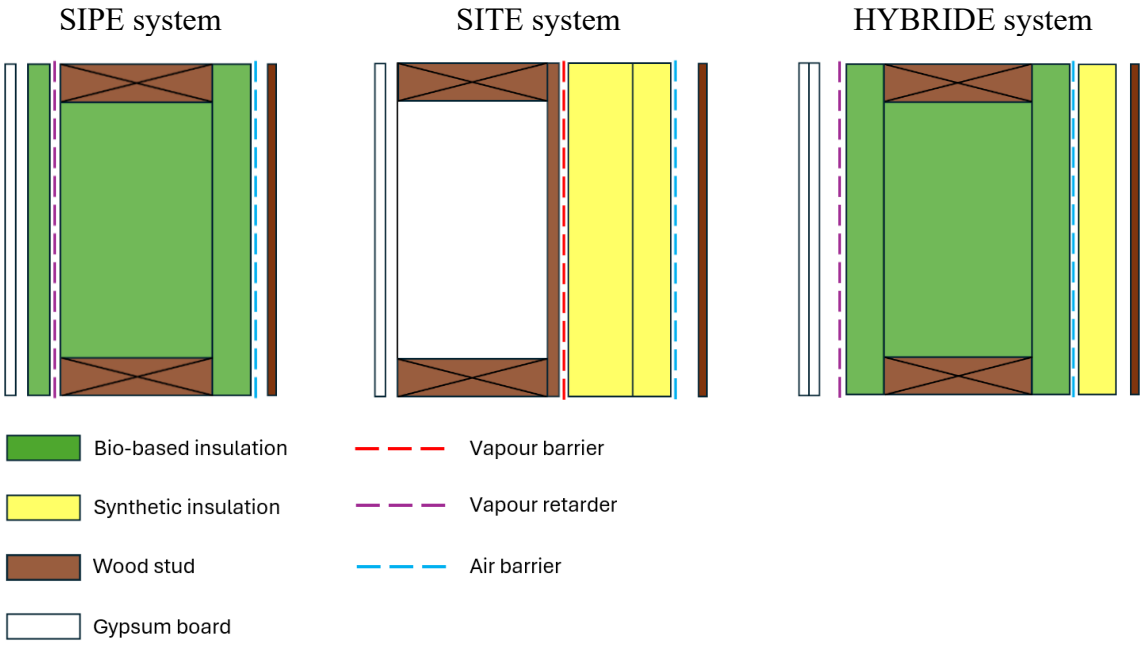

In-situ Assessment and Comparison of the Thermal Performance of Three Building Envelopes in a Nordic Climate

Luigiano Duarte,[a,b,*] Pierre Blanchet ,[a,*] Lara Ramadan,[b] and Richard Trempe [c]

Buildings in cold climates are often exposed to extreme weather events, including heatwaves and prolonged power outages. In this study, three lightweight experimental buildings were instrumented in Québec to assess their thermal resilience. Each building featured a different wall assembly insulated with bio-based materials. The dynamic thermal behavior was analyzed during winter heating interruptions and summer heatwaves, using *in situ* measurements and specific performance indicators. Although all three wall systems met high thermal resistance levels, results showed that this static property alone was not able to predict thermal resilience. One building, despite having lower static performance, maintained cooler indoor temperatures during a heat wave due to a higher share of bio-based materials. This study emphasizes the importance of moving beyond static indicators and relying on real-world performance assessments to inform sustainable building design in cold regions affected by climate change.

DOI: 10.15376/biores.21.1.1645-1668

Keywords: Sustainable building; Thermal inertia; Nordic climate; Bio-based materials; In-situ sensing

Contact information: a: Canada Research Chair on Sustainable Buildings (CRC-BD), Department of Wood and Forest Sciences, Université Laval, 2425 Rue De La Terrasse, Quebec City, QC G1V 0A6, Canada; b: LIMBHA, Ecole Supérieure du Bois (ESB), 7 rue Christian Pauc, 44300 Nantes, France; c: Trempe Architecte, 185 rue Paquet, Sainte-Christine-d'Auvergne (Québec) G0A 1AO;
Corresponding authors: luigiano.duarte.1@ulaval.ca; pierre.blanchet@sbf.ulaval.ca

INTRODUCTION

General Context

Climate change has become a central global concern, driving the development of political action. In 2016, Canada ratified the Paris Agreement and committed to reducing its greenhouse gas (GHG) emissions by 40 to 45% from 2005 levels by 2030 (Environment and Climate Change Canada 2025). The building sector accounts for 18% of Canada's GHG emissions. When including building materials and construction, it ranks as the third-largest source of emissions nationwide (Government of Canada 2020). These aspects makes it a key sector in the fight against climate change, highlighting the importance of reducing its GHG footprint.

Rising greenhouse gas emissions have significantly disrupted the global climate, increasing the frequency and intensity of extreme weather events such as heatwaves, droughts, and storms (Mora *et al*. 2018). According to the Intergovernmental Panel on Climate Change (IPCC 2021), global mean temperature could rise by 1.5 °C to 2 °C by the end of the 21st century. This warming trend is expected to amplify the frequency, intensity,

and duration of heatwaves. If emissions continue to rise, up to 74% of the world's population could be exposed annually to potentially deadly heatwaves by 2100 (Mora *et al*. 2017). Other extreme events, such as hurricanes and snowstorms, also directly threaten the reliability of energy infrastructure. They can trigger prolonged power outages lasting days, weeks, or even months (Wang *et al*. 2016). Climate disruption therefore has not only environmental consequences but also significant implications for thermal comfort.

In a Nordic climate such as Canada's, climate change may shorten the heating season while intensifying summer cooling demand. In Quebec City, depending on the type of building envelope, heating demand could decrease by 25% by 2080, whereas cooling demand could increase by 91 to 116% (Berardi and Jafarpur 2020; Piggot *et al*. 2025).

From a social perspective, people spend an average of 90% of their time indoors (Mannan and Al Ghamdi 2021). Indoor thermal comfort thus becomes a key factor for occupant well-being, health, and building energy performance (Kim *et al*. 2022). The combined intensification of heatwaves and power outages may severely compromise comfort, especially in the most vulnerable dwellings (Hampo *et al*. 2024; Hachem-Vermette and Yadav 2023).

Regulatory Context

To meet its greenhouse gas (GHG) reduction commitments, Canada has implemented strategic measures focused on promoting energy-efficient buildings. Improving the energy performance of both new and existing buildings, accounting for the embodied carbon of materials, and integrating construction processes during the design phase are key steps toward sustainable buildings (Conseil du bâtiment durable du Canada 2020).

In this context, the use of bio-based construction materials plays a key role in reducing the environmental footprint of the building sector (Pacheco-Torgal *et al*. 2025). Life cycle assessment studies in the construction industry have shown that bio-based construction solutions generally have lower environmental impacts than non-bio-based alternatives (Buyle *et al*. 2013; Cabeza *et al*. 2014). Recent research has highlighted the environmental advantages of hemp wool and wood fiber as bio-based insulating materials. In addition to being renewable, hemp wool offers a favorable carbon balance and excellent hygrothermal regulation capacity (Cosentino *et al*. 2023). Wood fiber is valued for its capacity to store carbon and its ability to mitigate greenhouse gas emissions associated with construction (Yang *et al*. 2020).

To ensure high energy performance, Canada relies on a structured regulatory framework based on national and provincial standards. The *National Energy Code for Buildings* (National Research Council of Canada 2018), in its 2020 edition, sets minimum energy efficiency requirements for new commercial, institutional, and industrial buildings. These include prescriptions on thermal insulation, airtightness, mechanical systems, and lighting performance (Government of Canada). In Quebec, the *Code de construction du Québec* adopts the *National Building Code of Canada* with province-specific amendments—notably Part 9.36 for residential buildings—to account for local climatic conditions (Régie du bâtiment du Québec 2022). In addition, the *Novoclimat 2.0* program, implemented by the Government of Québec, promotes the construction of buildings that exceed the minimum standard, with a focus on envelope quality, mechanical ventilation, and airtightness (Gouvernement du Québec 2022).

Minimum performance standards and building energy codes are becoming increasingly stringent worldwide, while efficient and renewable construction technologies are advancing rapidly (IEA 2023). Building energy performance depends mainly on the envelope's ability to limit heat transfer.

This limitation is generally assessed using a static indicator, such as thermal resistance (R-value or RSI, *R-value System International*), which measures a material or wall's ability to slow down heat flow under steady-state conditions. This approach underpins most current energy performance requirements. Improving the thermal resistance of envelope components—such as walls, roofs, and floors—through the use of thermal insulation reduces heat losses and, consequently, energy consumption (Kaynakli 2012; Asdrubali *et al*. 2013; Straube and Smegal 2009).

Recent analyses confirm that increasing the minimum thermal resistance (RSI) requirements for envelopes in codes such as the NECB 2020 and the Quebec version of the *National Building Code of Canada* (National Research Council of Canada 2022) is one of the most effective ways to reduce energy demand in cold climates (Régie du bâtiment du Québec 2022). As a result, many regulatory frameworks and programs, such as *Novoclimat 2.0* in Québec, set minimum RSI (or U-value) requirements, highlighting their central role in thermal building design.

In Québec and in the rest of Canada, two approaches are used to verify compliance with energy performance requirements. The Quebec version of the *National Building Code* (Chapter I – Building, modified for Quebec, latest version) still allows the use of either total thermal resistance (RSI-t), calculated from all wall layers with corresponding tables, or effective thermal resistance (RSI-e), which better reflects real installation conditions and thermal bridge effects. In contrast, the *National Energy Code for Buildings* (NECB) and several performance programs, such as *Novoclimat 2.0*, specifically require the use of effective thermal resistance (RSI-e), providing a more accurate representation of in-use performance (National Research Council of Canada 2020; Régie du Bâtiment du Québec 2022; TEQ 2022;).

However, as noted by Straube (2017), the R-value, while useful for its simplicity and wide adoption, is inadequate for predicting the actual thermal performance of assemblies, particularly under variable heat flow conditions or in the presence of construction defects. Thermal resistance is a static factor; it does not account for dynamic effects such as thermal lag and material heat capacity, which directly influence both thermal comfort and energy consumption (Verbeke and Audenaert 2018). R- and U-values are based on steady-state assumptions, which ignore temporal variations in climatic conditions or internal loads (Tian *et al.* 2021). In reality, heat transfer through walls is fundamentally transient, influenced by properties such as density, specific heat capacity, and thermal conductivity. This dynamic behavior is crucial for accurately estimating thermal loads, actual energy needs, and occupant comfort (Verbeke and Audenaert 2018).

For a more comprehensive assessment of thermal performance, dynamic models (transient simulations) or *in-situ* measurements are essential, as they can capture the real variations in use and climate (Wilde 2014; Tronchin and Fabbri 2008).

Thermal Inertia: A Dual Solution

Thermal inertia refers to a material or building's ability to store heat and release it later, in an attenuated and time-shifted manner, in response to outdoor temperature

variations or internal heat gains (Verbeke and Audenaert 2018). It acts as a thermal damping mechanism, particularly valuable in the context of climate change, as it slows down heat transfer through the envelope and helps stabilize indoor temperatures.

In buildings, this behavior primarily depends on the thermal mass, specific heat capacity, density, and thermal conductivity of the materials (Ascione *et al.* 2014). Massive materials such as brick or concrete are traditionally associated with high thermal inertia, but several recent studies have shown that some bio-based insulations—such as wood fiber or hemp wool—can also offer significant inertia, particularly due to their coupled hygrothermal properties (Palumbo *et al.* 2018).

Thermal inertia offers a twofold benefit. In summer, it reduces overheating amplitude by absorbing part of the solar gains. In winter, it slows down the cooling rate during heating interruptions. The magnitude of these effects, however, depends on the location of thermal mass within the wall assembly: interior layers provide greater benefits for indoor comfort, while external layers mainly act as a buffer against outdoor fluctuations. These properties are essential for thermal resilience—defined as the ability of a building to maintain a minimum level of comfort without active energy input (Verbeke and Audenaert 2018).

Several methods have been proposed in the literature to quantify building thermal inertia. Dynamic simulation approaches can provide indicators such as Time Lag and Amplitude Damping. These are typically derived from sinusoidal inputs in outdoor conditions, to assess the delay and reduction of indoor thermal peaks (Ascione *et al.* 2014). Other works rely on laboratory tests—such as thermal cells subjected to transient heat flux—to characterize the thermal response of materials or wall assemblies under controlled conditions (Carmona *et al.* 2023). At a more representative scale, *in-situ* experimental studies track indoor temperatures during critical events, such as heating outages or heatwaves, to capture the real-world impact of thermal inertia. Specific indicators, such as the Cooling Slope (CS) or Degree of Disturbance (DoD), have also been developed to characterize better the rate and magnitude of thermal variations in response to prolonged energy loss (Flores-Larsen *et al.* 2023). These approaches provide complementary tools to assess dynamic envelope performance.

Objectives and scope of the study

This study aimed to characterize the real thermal response of lightweight-frame buildings constructed with different insulating materials, in the context of climate change. It aimed to better understand how specific envelope parameters such as thermal inertia, and insulation type, impact thermal resilience during periods of environmental stress. The focus was on thermal comfort during power outages and overheating events, both of which are expected to become more frequent. The study provides an empirical contribution to the ongoing discussion on the real-world performance of buildings in a transitioning energy context.

Originality of the work

This research stands out for its full-scale experimental approach, conducted in a Nordic climate on high-energy-efficiency lightweight-frame buildings. It addresses thermal inertia not as a theoretical variable, but as a measurable resilience factor that directly influences the maintenance of thermal comfort in the absence of active energy

supply. The study critically examined commonly used indicators, such as effective thermal resistance, and explores more representative, dynamic alternatives.

By comparing three buildings with similar nominal R-values but differing in insulation materials, thermal mass, and airtightness, the study has potential to provide a clearer understanding of the relative influence of these parameters on actual thermal behavior. It delivers new experimental evidence to guide the design of buildings that are more resilient to extreme climate events. This work originated from Richard Trempe Architect's initiative to document and characterize the envelope performance of an innovative light wood-frame construction system.

EXPERIMENTAL SETUP AND METHODOLOGY

Buildings under Study

Three experimental buildings were specifically designed and constructed for this research. Initiated by Trempe Architecte in the region of Quebec, the project aimed to advance best practices in building envelopes for lightweight timber-frame construction. These buildings, named HERMINE, MARMONTIN, and SITELLE were located on the same site and subjected to strictly comparable environmental conditions: identical dimensions, orientation, fenestration with triple glazing, solar shading, ventilation systems, roof, floor, and ground conditions, as well as usage. All three buildings were built in compliance with the requirements of the *Novoclimat 2.0* program. The only variable between the three units was the composition of their exterior wall assembly, allowing the isolation of the envelope's effect on thermal inertia. A visual of one of the buildings is provided in Fig. 1 to illustrate the scale and architectural integration of the facilities.

Fig. 1. Photograph of the HERMINE (left), the SITELLE (center), and the MARMONTIN (wright)

The three wall assemblies corresponded to three construction systems: a *partially exterior-insulated system* (SIPE), a *fully exterior-insulated system* of the *perfect wall* type (SITE), and a hybrid system designed explicitly for this research. The assembly choices reflected contemporary practices aimed at improving energy efficiency while meeting regulatory requirements. Cross-sectional diagrams (Fig. 2a, b, c) illustrate the configuration of each wall, layer by layer. The selection of these assemblies was carefully considered during the project's preliminary phase.

Conventional system - SIPE (HERMINE)

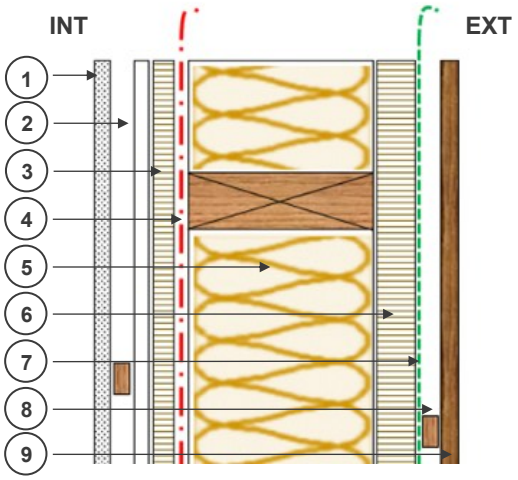

1 : Gypsum board (13 mm)
2 : Unventilated air gap (38 mm)
3 : Wood fiberboard (13 mm)
4 : Mbrain vapour retarder membrane
5 : 38x140mm studs filled with hemp wool
6 : ECO4 Wood fiberboard (38 mm)
7 : Tyvek air barrier membrane
8 : Ventilated air gap (13 mm)
9 : Wood siding (13 mm)

Fig. 2. Cross-section of the HERMINE wall assembly (SIPE)

The partially exterior-insulated system (SIPE), in Fig. 2, used in HERMINE is an optimized version of a configuration widely used to meet Novoclimat 2.0 requirements. It is based on a lightweight timber frame, typically with 2×4 in. or 2×6 in. studs filled with batt insulation (TEQ 2022). In this project, conventional materials (glass wool, mineral wool) were replaced with bio-based insulations that have higher specific heat capacities, such as hemp wool and wood fibre, to enhance thermal inertia (O'Brien *et al.* 2024). On the exterior of the framing, a continuous layer of rigid insulation (wood fibreboard) is added to reduce thermal bridging through the wooden studs. This layer improves the overall thermal resistance of the wall by maintaining insulation continuity, while also contributing to thermal buffering (Cabeza *et al.* 2014).

SITE System (SITELLE)

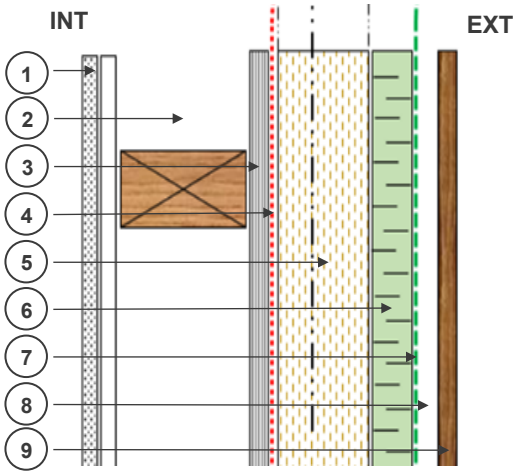

1 : Gypsum board (13 mm)
2 : Unventilated airgap (108 mm)
3 : Plywood pannel (13 mm)
4 : Self-adhesive RESISTO membrane
5 : Polyisocyanurate panel (64 mm)
6 : Isoclad panel EPS laminated (38 mm)
7 : Tyvek air barrier membrane
8 : Ventilated air gap (13 mm)
9 : Wood siding (13 mm)

Fig. 3. Cross-section of the SITELLE wall assembly (SITE)

The fully exterior-insulated system (SITE), in Fig. 3, implemented in SITELLE was inspired by the "perfect wall" by Lstiburek (2010). This configuration inverts the conventional logic of systems such as SIPE: all insulation is placed outside the structural frame, leaving the studs entirely on the warm side of the building, inside. This arrangement minimizes thermal bridging, increases the system's thermal inertia, and improves the stability of indoor conditions.

Unlike the other systems tested, SITE relies on synthetic insulation materials (notably Isoclad™ from Isolofoam™ and polyisocyanurate), both known for their high thermal performance (Jelle 2011). This configuration, developed specifically for this project, ensures air, vapour and water tightness by a continuous membrane between the intermediate sheathing and the insulation layer, enabling effective moisture management. While still uncommon in the residential sector, this system is widely used in institutional construction and in cold climates, where it provides complete protection of the timber structure against climatic variations.

SIPE System upgraded (MARMONTIN)

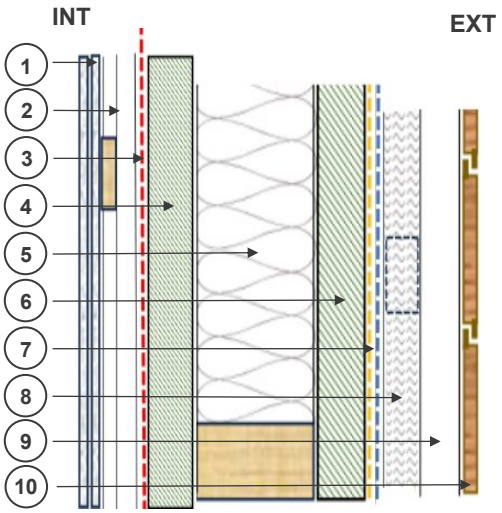

1 : Gypsum board (13 mm)
2 : Unventilated air gap (26 mm)
3 : Mbrain vapour retarder membrane
4 : ECO4 wood fiberboard (38 mm)
5 : 38x140 mm studs filled with hemp wool
6 : ECO4 wood fiberboard (38 mm)
7 : Tyvek air barrier membrane
8 : Comfortboard™ 80, a rigid stone wool insulation board (38 mm)
9 : Ventilated air gap (38 mm)
10 : Wood siding (13 mm)

Fig. 4. Cross-section of the MARMONTIN wall assembly (System upgraded)

The MARMONTIN system, in Fig. 4, is an evolution of the conventional SIPE configuration, designed to increase the wall's thermal inertia. Both HERMINE and MARMONTIN prioritized a high proportion of bio-based materials, but MARMONTIN was designed with greater mass to further enhance heat storage capacity. To achieve this, two interior gypsum boards are used instead of the standard single layer, and the interior wood fiberboard panel is replaced with a panel three times thicker. The thickness of hemp insulation between studs is reduced, but an exterior layer of mineral wool is added. This material, which is less hygroscopic than bio-based insulations, enhances the wall's resistance to moisture while maintaining its solid thermal performance.

In-situ buildings

Although the three assemblies exhibit slightly different thermal resistances due to the nature and arrangement of the insulating materials, all are considered high-energy-

performance systems. Each wall meets the requirements of the *Novoclimat 2.0 program*, confirming its effectiveness in thermal insulation, airtightness and its relevance for high-performance residential buildings in cold climates.

All three assemblies must comply with the requirements of the Quebec version of the *National Building Code* (Chapter I – Building, modified for Quebec 2020) and those of the *National Energy Code of Canada for Buildings* (NECB 2020), where applicable. However, the NECB does not apply to residential buildings with fewer than three storeys and a floor area of less than 600 m², in which case only the NBC 2020 applies.

The assemblies were designed to comply with the requirements of the Quebec version of the *National Building Code* and with the specifications of the *Novoclimat 2.0 program*. The table below (Table 1) presents the regulatory effective thermal resistance values required.

Table 1. Regulatory Requirements for Thermal Resistance in Residential Buildings in Climate Zone 7A

Criterion	Quebec version of the *National Building Code*	*Novoclimat 2.0 Program*
Type of thermal resistance	Effective	Effective
Minimum RSI requirement (m².K/W)	≥ 3.60	≥ 4.14
Equivalent R-Value (imperial)	R-20.4	R-23.5
Specificity	Part 9.36 – Residential buildings	Real conditions, stricter than the Code

The effective thermal resistances of the assemblies were determined through theoretical calculations. When HERMINE was built, the thermal resistance values for hemp were less reliable. They were overestimated, and this error allowed HERMINE to meet the requirements of the *Novoclimat 2.0* program.

Table 2. Theoretical and Measured Effective Thermal Resistances of the Different Assemblies

Criterion	HERMINE	MARMONTIN	SITELLE
Type of thermal resistance	Effective	Effective	Effective
RSI-e (m².K/W)	3.88	4.61	4.70

Blower-door tests were also conducted on all three buildings. The results expressed in air change rates at 50 Pa (ACH50) were 1.90/h for HERMINE, 1.65/h for SITELLE, and 0.67/h for MARMONTIN. Based on ACH50, only MARMONTIN meets the 1.5 threshold required by Novoclimat 2.0. Novoclimat 2.0 also accepts compliance through the standardized leakage area (SFN), with a limit of 0.75 cm²/m². According to this criterion, SITELLE reaches 0.62 cm²/m² and is therefore compliant, while HERMINE records 0.88 cm²/m² and remains above the threshold. In summary, only SITELLE and MARMONTIN meet Novoclimat 2.0 airtightness requirements. The unit cm²/m² expresses leakage area relative to the building envelope surface, allowing airtightness to be compared across buildings of different sizes.

Materials and Instrumentation

The studied walls are composed of materials with varied thermal properties, combining bio-based insulation (such as wood fiber), synthetic insulation (such as expanded polystyrene), and high-thermal-mass materials (such as solid wood). These compositions enable the exploration of various approaches to thermal performance, leveraging both insulating capacity and thermal inertia. All sensors were validated and calibrated in the lab prior to installation. Furthermore, temperature spot checks were performed using an IR thermometer throughout the test.

These physical properties, such as thermal conductivity, density, thickness, and specific heat capacity, were obtained from manufacturers' datasheets or the *EN10456-2012* database. All parameters are presented in Table 3, which details the thermal properties of each layer making up the different assemblies.

Table 3. Table Detailing the Physical Characteristics of the Different Materials

Material	Thermal conductivity	Density	Thickness	Specific heat capacity
	[m².K/W]	[kg/m³]	[mm]	[J/Kg.K]
Gypsum	0.1374	900	0.013	1090
Mineral wool 80	0.0353	80	0.038	1030
Hemp wool 89	0.0581	35	0.089	1700
Hemp wool 140	0.0581	35	0.140	1700
Wood fiber ECO4	0.0497	265	0.038	2100
Wood fiber standard	0.0442	110	0.013	2100
Polyisocyanurate	0.0292	35	0.064	1400
Isoclad	0.0343	40	0.038	1400

Thermocouples

Hobo MX1101 sensors were used to measure ambient temperature (AMB) with an accuracy of ±0.2 °C between −20 and 70 °C. For Hermine and Sitelle, wall thermocouples (Wall) were SmartReader Plus 6 (SRP6): ±0.2 °C from 0 °C to 70 °C, ±0.07 °C from −25 °C to 0 °C, and ±0.13 °C from −40 °C to −25 °C. For Marmontin, T9602-5-A sensors (Mouser, Digikey) were used, with an accuracy of ±0.5 °C between −20 and 70 °C. Outdoor temperature was recorded in a sheltered location near the buildings using an SRP6, with cross-checking against data from the Québec – Jean Lesage weather station. A deviation of ±0.4 °C between AMB and Wall readings indicates a significant difference; for Marmontin, this threshold was ±0.7 °C. This distinction was accounted for in the analysis to ensure data comparability and reliability across the three buildings.

Effective Thermal Resistance

Based on the thermal conductivities and the actual layer thicknesses, the effective thermal resistance (RSI-e) of each wall was calculated using the parallel heat flow method, which is recommended for wood-frame structures (Régie du bâtiment du Québec 2024). The equation used was,

$$\text{RSI-e}_{\text{parallel}} = \frac{100}{\frac{A_F}{RSI_F} + \frac{A_C}{RSI_C}} \quad (1)$$

where RSI-e is the effective thermal resistance of the complete assembly for compliance assessment, and A_F and A_C are the surface fractions occupied by the frame and the cavity. RSI_F and RSI_C are their respective thermal resistances. This method accounts for the effect of linear thermal bridges, which are typical of studs in light-frame walls. The calculated values were compared to the regulatory requirements of the Québec version of the *Canadian Building Code and the Novoclimat 2.0 program* (TEQ 2022).

In-situ Experimentation

Three experimental buildings—identical in dimensions, orientation, ventilation system, and usage—were built on the same site in Québec. Only their exterior wall composition differed: Hermine (SIPE), Sitelle (SITE), and Marmontin (Hybrid). Each building was instrumented in the same way to ensure strict comparability. A thermocouple was placed in each building at ground-floor level, both in the interior environment (AMB) and within the wall assembly (Wall). Sensors were positioned at identical locations in the three buildings. To minimize measurement bias, monitoring was conducted in north-facing zones to reduce sensitivity to solar radiation. A schematic diagram (Fig. 5) illustrates the spatial arrangement of the instrumentation, showing the location of AMB and Wall sensors.

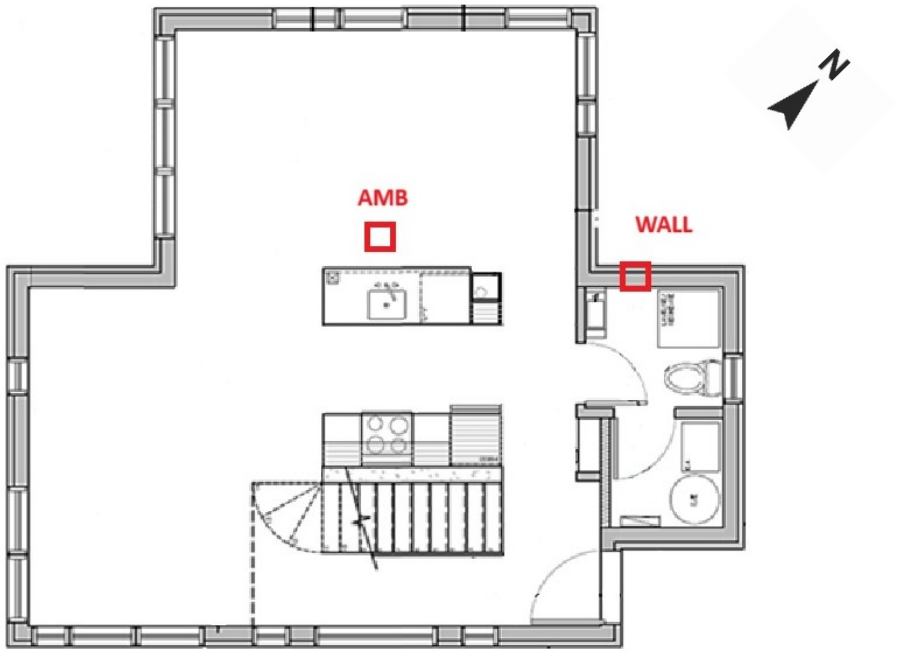

Fig. 5. Cross-sectional diagram of building instrumentation at ground-floor level, showing AMB and WALL thermocouples (author's illustration).

Winter Heating Outage

A planned heating outage was carried out simultaneously in the three experimental buildings described above during the middle of winter. The heating cut-off lasted nearly 80 hours between January 14 and 17, 2025. The initial indoor temperature was 21 °C ± 0,5 °C. Temperature data were collected every 15 minutes using thermocouples. These sensors were placed in two distinct locations: in the indoor ambient air (AMB) and at the inner

interface of the walls, just behind the gypsum board (WALL). Monitoring continued until a critical threshold of 5 °C was reached. As a precaution, the experiment was stopped before dropping below this threshold to avoid any risk of pipe damage. In addition, an outdoor probe was placed in a sheltered location to record the reference outdoor temperature throughout the experiment, ensuring accurate control of the climatic conditions.

In accordance with ASHRAE 55 recommendations for non-conditioned spaces, a comfort threshold of 18 °C was adopted. This 18 °C limit served as the reference point for evaluating the onset of thermal discomfort inside the buildings.

Several quantitative indicators were used to characterize the thermal resilience of the buildings during the winter power outage. These indicators are inspired by recent work (Hamdy *et al.* 2017; Flores-Larsen *et al.* 2023) on power outages. This section presents the various indicators used in the study.

Minimal temperature (T_{min})

T_{min} was used as an indicator of the lowest temperature reached during the outage. This value enabled the assessment of the maximum heat loss during the disruptive event.

Thermal resistance time (RT)

RT was also used to assess the time required for the indoor temperature to reach the 18 °C threshold. This parameter is defined in Eq. 2,

$$RT = t_{threshold} - t_0 \quad (2)$$

where $t_{threshold}$ is the time at which the measured temperature drops below the threshold temperature, and t_0 marks the start of the heating outage.

Intensity of the failure (IoF)

IoF was calculated to quantify the ability of the walls to resist thermal variation. This parameter is defined as follows in Eq. 3,

$$IoF = T_{initial} - T_{min} \quad (3)$$

where $T_{initial}$ is the initial temperature before the power outage, and T_{min} is the minimum temperature reached during the outage.

Cooling speed (CS)

CS was calculated to measure the rate at which the indoor temperature dropped after the heating shutdown. This metric assesses the effectiveness of materials in slowing down the cooling process. CS was obtained by taking the difference between the initial temperature and the minimum temperature reached, then dividing it by the duration of the outage. This parameter is defined in Eq. 4.

$$CS = \frac{T_{initial} - T_{min}}{t_{min} - t_0} \quad (4)$$

This indicator provides an estimate of the rate at which heat loss occurs in the building, which is essential for understanding the thermal responsiveness of the envelope.

Degree of disruption (DoD)

The DoD was calculated to quantify the thermal impact of the heating outage, using the comfort threshold of 18 °C. This parameter is defined in Eq. 5.

$$DoD = \frac{1}{D \cdot T_{threshold}} \int_0^D \max\left(0,\ T_{threshold} - T_{indoor}(t)\right) dt, \quad (5)$$

where D represents the duration in hours of the power outage, and the integral is taken over the period when the indoor temperature remains below this threshold. This calculation provides a dimensionless measure of the magnitude of the thermal disturbance. As the DoD increases, thermal resilience decreases.

Summer Overheating

The analysis focused on identifying the most intense summer heatwave events. These are sequences of several consecutive days during which the maximum outdoor temperature significantly exceeds seasonal normals. Although these periods do not necessarily meet Environment Canada's official heatwave criteria, they represent critical episodes from the standpoint of indoor thermal comfort. In the revised methodology, a comfort threshold of 25 °C was adopted (per ASHRAE 55 recommendations for naturally conditioned spaces). This 25 °C threshold served as the reference for assessing the onset of thermal discomfort inside the buildings. Thus, each heatwave was characterized by its start (when the outdoor temperature rises well above 25 °C) and its end (return to milder outdoor conditions), allowing the reaction of the buildings to be measured over the entire duration of the hot event. For external reasons, the experimental period was limited to May and June 2025 to ensure the buildings remained unoccupied.

Five thermal performance indicators were adopted for each building. Each was calculated separately from AMB (indoor) and WALL (in-wall) sensor data, in order to evaluate both the indoor air environment and the inertial response of the wall. These indicators are inspired by the recent work of Hamdy *et al*. (2017) on thermal resilience. In Hamdy's study, calculations were done by zones, which was not the case here. As a result, the formulas were simplified, as they did not take zoning into account.

Indoor overheating degree (IOD)

The IOD measures the intensity of a building's indoor overheating, expressed in °C·h. It quantifies the duration during which the indoor temperature exceeds a predefined comfort threshold. This parameter is defined as follows in Eq. 6:

$$IOD = \frac{1}{T_{outdoor}} \sum_{i=1}^{n} \max\left(0,\ T_{indoor}(t_i) - T_{threshold}\right) \cdot \Delta t \quad (6)$$

where $T_{outdoor}$ is the maximum outdoor temperature observed during the period, $T_{indoor}(t_i)$ is the sensor-measured indoor temperature at time t_i, $T_{threshold}$ is the comfort threshold of 25 °C, Δt is the time interval between each temperature measurement, and n is the total number of measurements taken during the period.

Ambient warmness degree (AWD)

The AWD measures the intensity of a building's indoor overheating, expressed in °C·h. It quantifies the duration during which the outdoor temperature exceeds a predefined comfort threshold. This parameter is defined as follows in Eq. 7,

$$AWD = \frac{1}{T_{outdoor}} \sum_{i=1}^{n} \max(0,\ T_{outdoor}(t_i) - T_{threshold}) \cdot \Delta t \quad (7)$$

where T_{ext} is the maximum outdoor temperature observed during the period, $T_{outdoor}(t_i)$ is the outdoor temperature measured at time t_i, $T_{threshold}$ is the comfort threshold of 25 °C, Δt is the time interval between each temperature measurement, and n is the total number of measurements taken during the period.

Overheating escalation factor (α_IOD)

The α_IOD factor determines the ratio of indoor overheating to outdoor overheating. This parameter is defined in Eq. 8.

$$\alpha_{IOD} = \frac{\Delta IOD}{\Delta AWD} \quad (8)$$

This methodology was applicable to short-term and long-term heat waves, as well as to annual overheating assessments.

Thermal amplitude

The amplitude measures the difference between the maximum and minimum temperatures, in °C. This parameter is defined as follows in Eq. 9,

$$Amplitude = T_{max,outdoor} - T_{max,indoor} \quad (9)$$

where $T_{max,\ outdoor}$ is the peak recorded outdoor temperature, and $T_{max,\ indoor}$ is the peak recorded indoor temperature.

Thermal phase shift (TPS)

TPS measures the time lag, in hours, between the peak outdoor temperature and the peak indoor temperature. It reflects the building's thermal inertia. This parameter is defined as follows in Eq. 10,

$$TPS = t_{max,\ indoor} - t_{max,\ outdoor} \quad (10)$$

where $t_{max,\ indoor}$ is the moment when the indoor temperature reaches its peak, and $t_{max,\ outdoor}$ is the moment when the outdoor temperature reaches its peak.

Data Processing and Visualization

Raw data were extracted using TrendReader 3 and ReDAQ Shape MAQ20 software. They were then organized and processed in Excel before being graphically analyzed with OriginPro. The analysis relied entirely on experimental data.

Thermal Comfort Assessment: Models and Indicators Used

Thermal comfort assessment in this study was based on temperature thresholds defined by ASHRAE Standard 55 (2021), which is recognized for its suitability in non-steady-state experimental situations. In line with this standard, the lower comfort threshold was set at 18 °C for winter, and the upper threshold at 25 °C for summer. These values served as reference points in calculating dynamic indicators such as thermal resistance time (RT), degree of disruption (DoD), and indoor overheating degree (IOD). In contrast, ISO 7730 (2005), based on Fanger's model, assumes a thermally homogeneous and mechanically ventilated environment, which did not correspond to the experimental

conditions of this study (Fanger 1970). ASHRAE Standard 55 (2021) allows the use of fixed operative temperature thresholds when data on radiation, humidity, and air speed are unavailable or irrelevant, particularly during short-term thermal drifts or when radiative asymmetries are minimal. Since measurements were taken in indoor spaces without major radiative gradients, air temperature was used as an approximation of operative temperature, in line with practices adopted in other studies in Nordic climates.

RESULTS AND DISCUSSION

Power Outage

Figure 6 shows the AMB temperature profiles of the three buildings during the power outage.

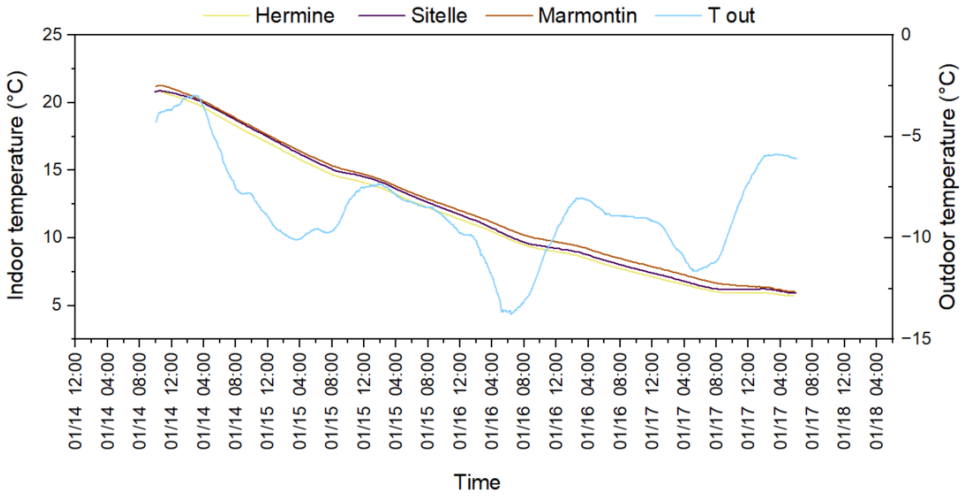

Fig. 6. Evolution of indoor temperatures during the heating outage from January 14 to 17, 2025

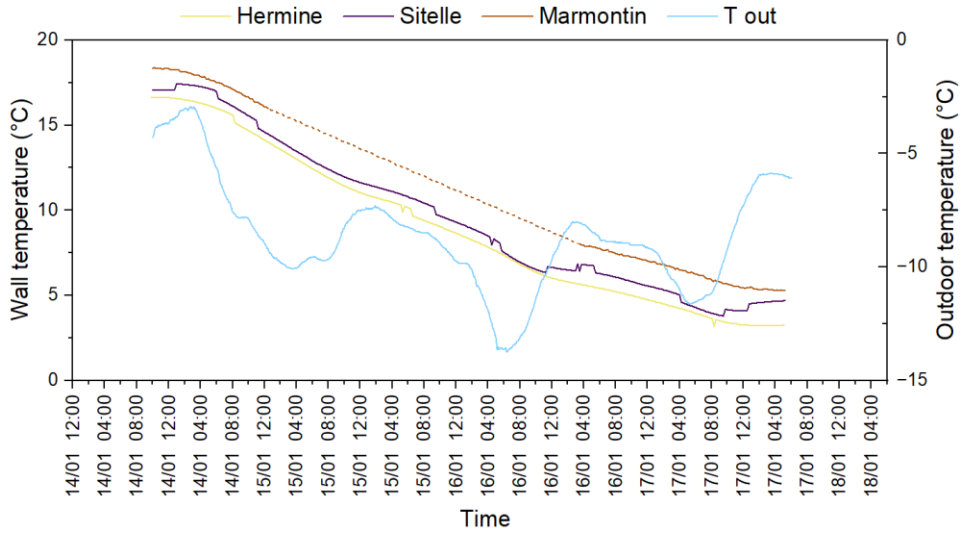

Fig. 7. Evolution of walls temperatures during the heating outage from January 14 to 17, 2025

The three buildings followed each other closely and displayed similar behavior in terms of the evolution of their AMB temperatures. The decline in indoor temperatures was steady, and variations in outdoor temperatures did not seem to influence AMB temperatures significantly.

Figure 7 shows the WALL temperature profiles of the three buildings during the power outage. Unlike the AMB temperatures in Fig. 6, the WALL temperatures did not start from the same initial point.

All three buildings exhibited similar temperature drops. An unforeseen issue occurred during testing, resulting in missing data for Marmontin from approximately 3 p.m. on January 15 to 4 a.m. on January 16. These values were smoothed through interpolation. According to the data acquisition in the other buildings, temperature variation was steady and monotonic during this period, ensuring negligible impact on the results. It can also be noted that Sitelle's wall temperature showed phases of instability, which was not observed in Hermine or Marmontin. This instability may be related to the position of the thermocouple within Sitelle's air cavity, where convective air movements can induce local temperature fluctuations. The target setpoint temperature was 21 °C, and the resilience threshold ($T_{threshold}$) was 18 °C. The results are summarized in Table 4. They are also compared with those from Gortych and Kuczyński (2025) to draw on another very similar *in-situ* study, but with different wall compositions. The average outdoor temperatures were relatively close, at −8.7 °C during th*is experimentation*, and −5.5 °C during the simulation by Gortych *et al.* (Gortych and Kuczyński 2025).

Table 4. Thermal Resilience Indicators during the Power Outage

	RT	IoF	CS	DoD	T_{min}	$T_{ext\ mean}$
	[h]	[°C]	[°C/h]	[-]	[°C]	[°C]
$Hermine_{AMB}$	10.5	15.1	0.191	0.363	5.72	-8.7
$Sitelle_{AMB}$	11.8	14.9	0.189	0.350	5.85	-8.7
$Marmontin_{AMB}$	12.3	15.3	0.193	0.333	6.03	-8.7
$Hermine_{wall}$	-	13.9	0.175	0.508	3.19	-8.7
$Sitelle_{wall}$	-	12.8	0.163	0.459	3.78	-8.7
$Marmontin_{wall}$	-	13.1	0.165	0.382	5.23	-8.7
Light-$frame_{AMB}$ [Gortych *et al.*]	8.0	15.0	0.109	0.526	6.5	-5.5
Heavy-$frame_{AMB}$ [Gortych *et al.*]	11.0	8.5	0.062	0.305	13.0	-5.5

The AMB temperature drop results were relatively similar across the three buildings. The RT values show that it took approximately 10 to 12 hours for each building to drop below the resilience threshold of 18 °C. Regarding IoF, CS, and DoD, the results were significantly close, indicating that all three buildings exhibited very similar thermal resilience in terms of AMB temperature evolution.

For wall temperatures, the IoF indicated comparable behavior between Hermine, Sitelle, and Marmontin. In contrast, the CS values were notably different: Hermine showed a cooling rate of 0.175 °C/h, while Sitelle and Marmontin cooled more slowly at 0.163 °C/h and 0.165 °C/h, respectively, with Marmontin cooling 20% slower than Hermine. The degree of disruption was highest for Hermine (0.508), while Sitelle (0.459) and Marmontin (0.382) performed better, with Marmontin's DoD being 33% lower than Hermine's.

However, DoD comparison must be interpreted cautiously here, as initial temperatures differed significantly: Hermine started at 17.05 °C, Sitelle at 16.62 °C, and Marmontin at 18.33 °C. A direct comparison of DoD between WALL and AMB readings was not possible due to these initial temperature differences. Nevertheless, the IoF values for the WALL sensors were consistently lower than those for the interior environment.

When comparing RT values with Gortych *et al*.'s light-frame building, their assembly took 8 hours to drop from 21 to 18 °C, whereas the wood-frame assemblies here required 10.5 to 12.3 hours, despite more adverse outdoor temperatures for Hermine, Sitelle, and Marmontin. Based on IoF and Tmin, however, light-frame buildings were relatively similar to each other.

The results obtained were compared with those of previous *in-situ* studies, notably those by Marta Gortych and Tadeusz Kuczyński (Gortych and Kuczyński 2025), who used similar indicators to assess the thermal resilience of buildings under heating outage or energy interruption conditions. Gortych *et al*. (2025) compared the thermal behavior of two residential buildings — one with a light-frame timber structure and the other with a heavy-frame structure — in winter climate conditions. These values will be used to evaluate and compare the performance of the buildings in this study under similar climatic conditions.

Comparing the high-performance assemblies (Hermine, Sitelle, and Marmontin) with Gortych *et al*.'s heavy-frame assembly showed similar RT values. IoF differed substantially: the heavy-frame building showed a failure magnitude of 8.5 °C with a Tmin of 13 °C, indicating significantly better performance than the buildings in this study. Unfortunately, outdoor mean temperatures were notably different, and Gortych *et al*.'s (2025) outage duration was twice as long, making CS and DoD indicators too dissimilar for direct comparison.

Summer overheating

Figure 8 shows the temperature profiles from the AMB sensors of the three buildings during the overheating period.

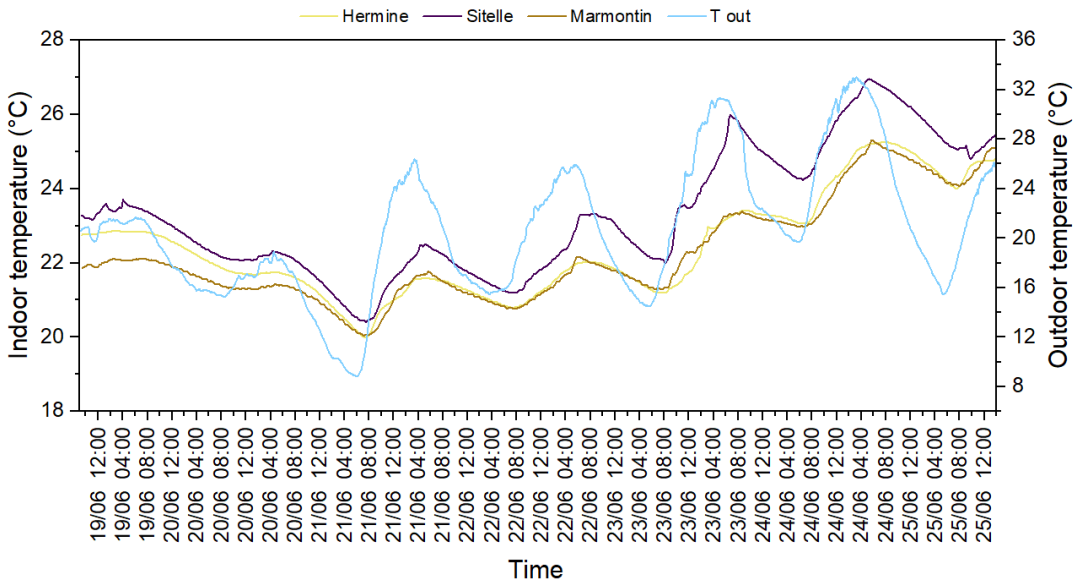

Fig. 8. Evolution of indoor temperatures during the heatwave from June 19 to 25, 2025

The AMB temperatures started at different values depending on the building: around 23 °C for HERMINE and SITELLE, and 22 °C for MARMONTIN. Outdoor temperatures ranged from 19 °C to 33 °C, with the heatwave beginning on June 21 and briefly exceeding 25 °C over the 4-day observation. HERMINE and MARMONTIN display similar, smooth, and controlled variations, while SITELLE showed a more irregular profile, with peaks approaching 27 °C. Figure 9 shows the WALL temperature profiles of the three buildings during the same period. The graph under Fig. 7 shows the WALL temperature profiles of the three buildings during the same period. WALL temperatures started at noticeably different levels, roughly between 21 and 23 °C. Unlike the indoor temperature trends (Fig. 6), Hermine and Marmontin displayed different behaviors. Sitelle remained the warmest wall assembly, reaching temperatures close to 27 °C. Hermine consistently recorded the coolest wall temperature and showed the highest resilience to the heatwave.

Table 5 presents the thermal resilience indicators during the heatwave. The AMB results for Hermine and Marmontin show extremely low IOD and αIOD values. While Sitelle also had low values, they were significantly higher compared to the other two buildings. This indicates that Hermine and Marmontin provided better comfort than Sitelle. Hermine and Marmontin also exhibited greater thermal amplitude. However, the two buildings differed in their phase shift: Hermine had a phase shift of approximately 4 hours, while Marmontin, like Sitelle, exhibited a phase shift of around 2 hours.

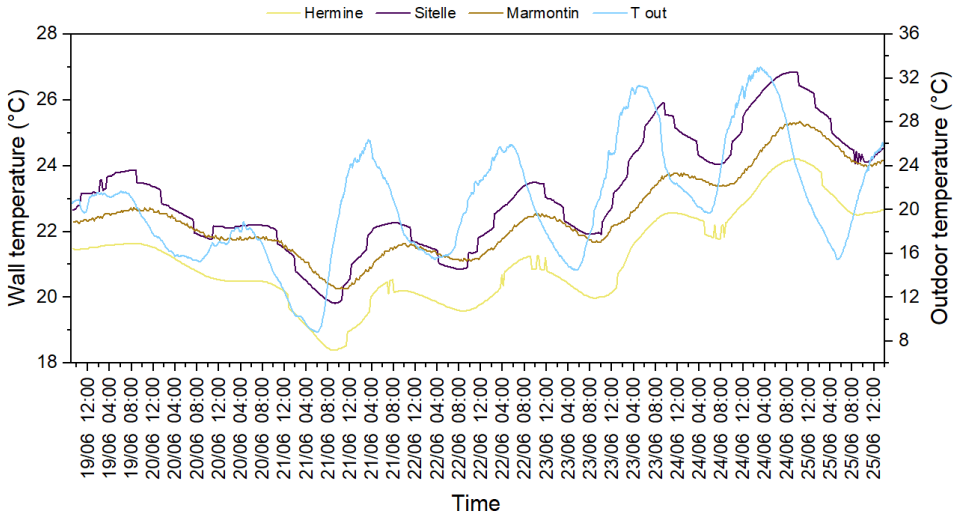

Fig. 9. Evolution of walls temperatures during the heatwave from June 19 to 25, 2025

Table 5. Thermal Resilience Indicators during the Heatwave

	IOD	AWD	αIOD	Amplitude	TPS	$T_{max\ Indoor}$
	[°C]	[°C]	[-]	[°C]	[h]	[°C]
$Hermine_{AMB}$	0.014	1.1	0.013	7.74	4.23	25.26
$Sitelle_{AMB}$	0.268	1.1	0.247	6.04	2.20	26.96
$Marmontin_{AMB}$	0.007	1.1	0.007	7.69	2.32	25.31
$Hermine_{wall}$	0	1.1	0	8.80	5.63	24.20
$Sitelle_{wall}$	0.228	1.1	0.209	6.14	5.33	26.86
$Marmontin_{wall}$	0.016	1.1	0.015	7.65	7.22	25.35

Regarding the WALL temperatures, the results were generally like those of the AMB, except that Sitelle's IOD and αIOD were lower. As for the amplitude, Hermine increased its temperature difference with the exterior, as its peak temperature decreased by one degree compared to the AMB. The amplitudes for Sitelle and Marmontin remained identical to the AMB temperatures. The significant difference between the AMB and WALL temperature variations during the June 24 heatwave was the phase shift. Hermine's phase shift increased from 4.23 to 5.63 hours, Sitelle's from 2.20 to 5.33 hours, and Marmontin's from 2.32 to 7.32 hours. These are highly significant observations, as they demonstrate that the exterior wall assemblies in all three buildings contributed to better thermal phase shift. It should also be noted that the different paint colors of the buildings likely influenced daytime thermal gains, with Hermine's white façade consistent with the lower heat absorption observed during the heatwave.

Main Differences between the Three Buildings

The effective thermal resistance is one of the key thermal characteristics of the opaque walls of Hermine, Sitelle, and Marmontin. All three walls are high-performance, although the measured effective thermal resistance of Hermine is slightly lower than that of the other two. The types of insulation used also differ. While Sitelle is insulated with synthetic materials, Hermine and Marmontin use bio-based materials such as hemp wool and wood fibre — Hermine containing more hemp wool, and Marmontin compensating with a greater proportion of wood fibre. All three assemblies are light-frame wood constructions, for which low thermal mass is an inherent limitation. Marmontin was the heaviest of the three, and Sitelle the lightest.

Power outage

The results obtained during the winter heating outage revealed a relative homogeneity in ambient temperatures among the three buildings, with a resistance time (RT) ranging from 10 to 12 hours before dropping below the 18 °C threshold. This apparent stability, however, conceals more marked differences in the temperatures measured within the exterior wall assemblies (WALL) and in dynamic indicators such as the cooling speed (CS) and the degree of disturbance (DoD).

Among the three tested assemblies, Marmontin's wall displayed the slowest cooling rate. This could be explained by the fact that Marmontin has the most massive wall construction, with the best insulation and the highest airtightness. Indeed, it is important to note that thermal inertia cannot be considered independently of air infiltration. Uncontrolled air exchange through the envelope disrupts the expected buffering effect, notably by accelerating heat gains or losses. Several studies (Miszczuk *et al.* 2020) emphasize the importance of combining thermal inertia with airtightness to enhance thermal resilience. These observations are consistent with the findings of Ascione *et al*. (2014), who highlight the role of thermal mass in damping indoor temperature fluctuations under transient conditions.

The wall of Sitelle, although lighter than that of Hermine, also showed a lower cooling rate. This behaviour could be due to its SITE-type configuration, in which the insulation is placed continuously on the exterior of the structure, or to its higher effective thermal resistance. This observation aligns with the principles outlined by Lstiburek regarding walls with continuous exterior insulation, although it does not allow for a

definitive conclusion. Further investigation is required.

Analysis of the DoD, in turn, revealed more pronounced differences between the buildings. Marmontin, with a lower DoD than Hermine and Sitelle, appeared to retain heat more effectively over time. However, the initial temperature differences between the buildings make direct comparison difficult. Since the DoD is an integrated indicator that strongly depends on starting conditions, it presents a certain methodological fragility, already noted by Zeng *et al*. (2022). It would therefore be preferable to combine this indicator with others, such as the minimum temperature reached or the duration spent below a given comfort threshold.

Overall, these results show that dynamic thermal performance cannot be attributed to a single factor such as thermal mass. Layer arrangement, type of insulation, and airtightness also interact in complex ways. Moreover, the differences observed within the walls are not always reflected in the ambient temperatures, suggesting that elements that remain unchanged between the buildings (such as windows, roofs, and floors) may play a decisive role in overall thermal behavior (Ascione *et al.* 2014).

Summer overheating

During the summer period, the performance differences between the three wall assemblies appeared more pronounced. The AMB values showed that Hermine and Marmontin withstood peak heat conditions better than Sitelle, with smoother temperature curves, more moderate maximum values, and lower IOD and αIOD indices. The performance of Hermine, despite having a measured Rtheff value lower than the other two, raises interesting questions about the relevance of thermal resistance in overheating situations.

Marmontin, although more massive, displayed slightly less favourable thermal behaviour than Hermine. This result may seem paradoxical, but it is possible that its high level of airtightness limited natural night-time ventilation, preventing the dissipation of heat accumulated during the day. Solgi *et al.* (2018) have shown that the absence of night cooling can exacerbate summer overheating, even in well-insulated envelopes. The interaction between airtightness and ventilation thus represents a particular point of attention, especially in passive or highly energy-efficient buildings.

Regarding the thermal time lag between Hermine and Marmontin, Marmontin's superior wall performance can be explained by its high airtightness and greater thermal mass. However, Hermine's better time lag performance in the indoor environment raises questions about the origin of this difference. Factors such as moisture content, layer arrangement, and the ability of indoor air to dissipate heat may also be influential variables, which are difficult to measure in a protocol limited to temperature data. This issue would warrant more in-depth laboratory testing.

The Sitelle wall, insulated with synthetic low-inertia materials, logically showed a more reactive thermal response, with greater amplitudes and higher temperature peaks. This behaviour is consistent with the characteristics of the materials used, which are less suited to storing heat but effective at limiting heat loss in winter. However, the possible influence of hygric inertia on thermal inertia could also partly explain Sitelle's observed performance.

The performance observed in this study suggests that bio-based materials, within the context of this research, may offer an effective and natural solution for summer comfort.

However, the performance differences between the buildings indicate that further research is needed to isolate the respective effects of each parameter, particularly through tests conducted under controlled laboratory conditions.

This study is part of an exploratory approach aimed at better identifying the conditions that promote the thermal resilience of lightweight timber-frame buildings in a Nordic climate. It provides evidence supporting certain principles (the value of thermal inertia, the structuring role of wall configuration) while also highlighting uncertainties and avenues for further research to optimise overall thermal performance.

CONCLUSIONS

1. Effective thermal resistance (RSI-e) is not a sufficient indicator for predicting the dynamic performance of opaque walls. While essential for limiting heat losses, it does not allow for anticipating a building's response to rapid climatic variations, particularly during heating outages or heatwaves.
2. Thermal mass and specific heat capacity appear to play a favourable role in slowing heat transfer in winter. However, this observation did not translate into better performance in summer.
3. The complementarity of bio-based materials, thermal mass, and layer arrangement should be studied in a more isolated manner, through dedicated experiments or simulations. The present real-world study highlights these interactions but cannot fully disentangle them.
4. The effect of airtightness cannot be conclusive in this study. While good airtightness improves heat retention in winter, it may limit heat dissipation in summer without appropriate ventilation. This aspect warrants further investigation.
5. Differences observed in wall temperatures do not systematically result in differences in indoor air temperatures, underlining the role of unmodified envelope components between buildings (windows, roofs, floors) in global thermal regulation, especially in winter.
6. The indicators used have limitations. The Degree of Disturbance (DoD) is highly dependent on the initial temperature, limiting its usefulness for cross-comparisons. Thermal resistance time (RT) and cooling speed (CS), while relevant for simplified assessments, do not fully capture the complexity of dynamic phenomena at the building scale.
7. The observation of this study should be explained in more detail with numerical simulation, especially regarding the dynamic behavior of biobased materials. Lab tests should be completed for this study to reduce variability and improve robustness.
8. The study could benefit from a completed life cycle analysis to complete the study.
9. This work provides valuable insights into the limitations of static insulation indicators and highlights the advantages of dynamic evaluation under real-world conditions.

ACKNOWLEDGMENTS

The authors acknowledge the Canada Research Chairs program (CRC-2022-00114), the Natural Sciences and Engineering Research Council of Canada (NSERC) discovery grant program (RGPIN-2021-03487), Zetco inc., the Quebec Housing Society (SHQ) Support Program for the Development of Quebec's Housing Industry (PADIQH), and the administrative and technical staff at the Research Center on Renewable Materials (CRMR).

REFERENCES CITED

Agence Internationale de l'Énergie (AIE). (2023). *Energy Efficiency 2023: Analysis and Outlook to 2030,* International Energy Agency, Paris, France.

American Society of Heating, Refrigerating and Air-Conditioning Engineers (ASHRAE) (2017). *ASHRAE Handbook – Fundamentals (SI edition)*, Atlanta, GA, USA.

ANSI/ASHRAE Standard 55 (2021). "Thermal environmental conditions for human occupancy," American Society of Heating, Refrigerating and Air-Conditioning Engineers, Atlanta, GA, USA.

Ascione, F., Bianco, N., De Masi, R. F., Mauro, G. M., and Vanoli, G. P. (2014). "Energy refurbishment of existing buildings through the use of phase change materials: Energy savings and indoor comfort in the cooling season," *Applied Energy* 190, 281-295. https://doi.org/10.1016/j.apenergy.2013.08.045

Asdrubali, F., Baldassarri, C., and Fthenakis, V. (2013). "Life cycle analysis in the construction sector: Guiding the optimization of conventional Italian buildings," *Energy and Buildings* 90, 65-75. https://doi.org/10.1016/j.enbuild.2013.04.018

Berardi, U., and Jafarpur, P. (2020). "Assessing the impact of climate change on building heating and cooling energy demand in Canada," *Renewable and Sustainable Energy Reviews* 121, article e109681. https://doi.org/10.1016/j.rser.2019.109681

Buyle, M., Braet, J., and Audenaert, A. (2013). "Life cycle assessment in the construction sector: A review," *Renewable and Sustainable Energy Reviews* 26, 379-388. https://doi.org/10.1016/j.rser.2013.05.001

Cabeza, L. F., Rincón, L., Vilariño, V., Pérez, G., and Castell, A. (2014). "Life cycle assessment (LCA) and life cycle energy analysis (LCEA) of buildings and the building sector: A review," *Renewable and Sustainable Energy Reviews* 29, 394-415. https://doi.org/10.1016/j.rser.2013.08.037

Carmona, C., Muñoz, J., and Alorda-Ladaria, B. (2023). "Ambient hot box: An instrument for thermal characterization of building elements and constructive materials," *Sensors* 23(3), article 1576. https://doi.org/10.3390/s23031576

Conseil du Bâtiment Durable du Canada (2020). *Plan Stratégique 2020–2025*, Montréal, QC, Canada (https://cbdc.org/plan-strategique-2020-2025/).

Conseil National de Recherches du Canada (2020). *Code National de L'énergie pour les Bâtiments – Canada 2020 (CNÉB 2020),* Gouvernement du Canada, Ottawa, ON, Canada.

Cosentino, L., Cantón, T., and De Castro, P. (2023). A review of natural bio-based insulation materials: Thermal and environmental insights. Energies, 16(12), article

4676. https://doi.org/10.3390/en16124676
Environnement et Changement Climatique Canada (2025). *Indicateurs Canadiens de Durabilité de L'environnement: Émissions de Gaz à Effet de Serre (Édition de 2025)*, Gatineau, QC, Canada.
Fanger, P. O. (1970). *Thermal Comfort: Analysis and Applications in Environmental Engineering*, Danish Technical Press, Copenhagen, Denmark.
Flores Larsen, S., Filippín, C., and Bre, F. (2023). "New metrics for thermal resilience of passive buildings during heat events," *Renewable and Sustainable Energy Reviews* 178, article 113220. https://doi.org/10.2139/ssrn.4288177
Gortych, M., and Kuczyński, T. (2025). "Winter thermal resilience of lightweight and ground coupled mediumweight buildings: An experimental study during heating outages," *Energies* 18(15), article 4022. https://doi.org/10.3390/en18154022
Hachem-Vermette, C., and Yadav, S. (2023). "Impact of power interruption on buildings and neighborhoods and potential technical and design adaptation methods," *Sustainability* 15(21), article 15299. https://doi.org/10.3390/su152115299
Hamdy, M., Liu, X., Bomberg, K., and Hicks, B. (2017). "The impact of climate change on the overheating risk in dwellings – A Dutch case study," *Building and Environment* 122, 307-323. https://doi.org/10.1016/j.buildenv.2017.06.031
Hampo, C. C., Schinasi, L. H., and Hoque, S. (2024). "Surviving indoor heat stress in the United States: A comprehensive review exploring the impact of overheating on the thermal comfort, health, and socioeconomic factors of occupants," *Heliyon* 10(3), article e25801. https://doi.org/10.1016/j.heliyon.2024.e25801
Intergovernmental Panel on Climate Change (IPCC) (2021). *Climate Change 2021: The Physical Science Basis*, Geneva, Switzerland.
ISO 10456 (2007). "Building materials and products – Hygrothermal properties – Tabulated design values and procedures for determining declared and design thermal values," International Organization for Standardization, Geneva, Switzerland.
ISO 7730 (2005). "Ergonomics of the thermal environment – Analytical determination and interpretation of thermal comfort using calculation of the PMV and PPD indices and local thermal comfort criteria," International Organization for Standardization, Geneva, Switzerland.
Jelle, B. P. (2011). "Traditional, state-of-the-art and future thermal building insulation materials and solutions—Properties, requirements and possibilities," *Energy and Buildings* 43(10), 2549-2563. https://doi.org/10.1016/j.enbuild.2011.05.015
Kaynakli, Ö. (2012). "A review of the economical and optimum thermal insulation thickness for building applications," *Renewable and Sustainable Energy Reviews* 16(1), 415-425. https://doi.org/10.1016/j.rser.2011.08.006
Kim, Y. K., Abdou, Y., Abdou, A., and Altan, H. (2022). "Indoor environmental quality assessment and occupant satisfaction: A post-occupancy evaluation of a UAE university office building," *Buildings* 12(7), article 986. https://doi.org/10.3390/buildings12070986
Lstiburek, J. W. (2010). *BSI 001: The Perfect Wall*, Building Science Corporation, Westford, MA, USA.
Mannan, M. M., and Al Ghamdi, S. (2021). "Indoor air quality in buildings: A comprehensive review on the factors influencing air pollution in residential and commercial structures," *International Journal of Environmental Research and Public*

Health 18(6), article 3276. https://doi.org/10.3390/ijerph18063276

Miszczuk, K., Sobczak-Piąstka, J., and Nowak, A. (2020). "Impact of airtightness on the building's energy demand in different climate zones," *Energies* 14(1), article 127. https://doi.org/10.1051/matecconf/201711700120

Mora, C., Dousset, B., Caldwell, I., Powell, F. E., Geronimo, R. C., Bielecki, C. R., Counsell, C. W. W., Dietrich,, B., Johnston, E. T., Louis, L. V., *et al.* (2017). "Global risk of deadly heat," *Nature Climate Change* 7, 501-506. https://doi.org/10.1038/nclimate3322

Mora, C., Spirandelli, D., Franklin, E. C., Lynham, J., Kantar, M. B., Miles, W., Smith, C. Z., *et al.* (2018). "Broad threat to humanity from cumulative climate hazards intensified by greenhouse gas emissions," *Nature Climate Change* 8(12), 1062-1071. https://doi.org/10.1038/s41558-018-0315-6

National Research Council Canada (NRCC). (2022). *National Building Code of Canada 2020, 2022 Revisions*, Canadian Commission on Building and Fire Codes, Ottawa, ON, Canada.

National Research Council of Canada (2020). *National Energy Code of Canada for Buildings 2020,* NRC Publications, Ottawa, ON, Canada.

O'Brien, L., Keller, M., and Lützkendorf, T. (2024). "Review of bio-based wood fiber insulation for building envelopes: Characteristics and performance assessment," *Energy and Buildings* 279, article 112624. https://doi.org/10.1016/j.enbuild.2024.115114

Pacheco Torgal, F., Ivanov, V., and Tsang, D. C. W. (eds.). (2025). *Advances in Bio-Based Materials for Construction and Energy Efficiency*, Woodhead Publishing, Cambridge, UK.

Palumbo, M., Lacasta, A. M., Giraldo, M. P., Haurie, L., and Correal, E. (2018). "Bio-based insulation materials and their hygrothermal performance in a building envelope system (ETICS)," *Energy and Buildings* 174, 147-155. https://doi.org/10.1016/j.enbuild.2018.06.042

Piggot Navarrete, J., Blanchet, P., Cabral, M.-R., and Cogulet, A. (2025). "Impact of climate change on the energy demand of buildings utilizing wooden prefabricated envelopes in cold weather," *Energy and Buildings* 338, article 115714. https://doi.org/10.1016/j.enbuild.2025.115714

Régie du bâtiment du Québec (2022). *Code de Construction du Québec, Chapitre I – Bâtiment et Code National du Bâtiment – Canada 2015 (modifié). Partie 11 – Efficacité Énergétique des Bâtiments Résidentiels*, Gouvernement du Québec, Québec, Canada.

Régie du bâtiment du Québec (RBQ). (2024). *Guide Technique sur la Performance Thermique des Murs à Ossature Bois*, Gouvernement du Québec, Québec, Canada.

Ressources Naturelles Canada (2020). *Stratégie Canadienne pour les Bâtiments Verts: Feuille de Route Vers des Bâtiments à Émissions Nettes Nulles*, Gouvernement du Canada, Ottawa, ON, Canada.

Solgi, E., Hamedani, Z., Fernando, R., Skates, H., and Orji, N. E. (2018). "A literature review of night ventilation strategies in buildings," *Energy and Buildings* 173, 337-352. https://doi.org/10.1016/j.enbuild.2018.05.052

Straube, J. F. (2007). "The passive house standard in North American climate zones," *ASHRAE Transactions* 113(1), 640-648.

Straube, J., and Smegal, J. (2009). *Building America Special Research Project: High R-value Enclosure Assemblies*, Building Science Corporation Report, Building Science Corporation, Somerville, MA, USA.

Transition énergétique Québec (TEQ). (2022). *Programme Novoclimat – Guide Technique – Habitations Unifamiliales*, Gouvernement du Québec, Québec, Canada.

Tronchin, L., and Fabbri, K. (2008). "Energy performance building evaluation in Mediterranean countries: Comparison between software simulations and real data," *Energy and Buildings* 40(7), 1176-1187. https://doi.org/10.1016/j.enbuild.2007.10.012

Verbeke, S., and Audenaert, A. (2018). "Thermal inertia in buildings: A review of impacts across climate and building use," *Renewable and Sustainable Energy Reviews* 82, 2300-2318. https://doi.org/10.1016/j.rser.2017.08.083

Wilde, P. (2014). "The gap between predicted and measured energy performance of buildings: A framework for investigation," *Automation in Construction* 41, 40-49. https://doi.org/10.1016/j.autcon.2014.02.009

Wang, Y., Chen, C., Wang, J., and Baldick, R. (2016). "Research on resilience of power systems under natural disasters—A review," *IEEE Transactions on Power Systems* 31(2), 1604-1613. https://doi.org/10.1109/TPWRS.2015.2429656

Yang, W., Keller, M., and Lützkendorf, T. (2020). "Life cycle assessment of wood-based insulation materials in building construction," *Journal of Cleaner Production* 258, article 120352. https://doi.org/10.17423/afx.2018.60.1.16

Zeng, Z., Zhang, W., Sun, K., Wei, M., and Hong, T. (2022). "Investigation of pre-cooling as a recommended measure to improve residential buildings' thermal resilience during heat waves," *Building and Environment* 210, article 108694. https://doi.org/10.1016/j.buildenv.2021.108694

Article submitted: September 3, 2025; Peer review completed: September 28, 2025;
Revised version received: November 26, 2025; Accepted: November 30, 2025;
Published: January 8, 2026.
DOI: 10.15376/biores.21.1.1645-1668